European Journal of
Mineralogy
Open Access

Bobtraillite from Gejiu hyperagpaitic nepheline syenite, southwestern China: new occurrence and crystal structure

Yanjuan Wang[1,2], Fabrizio Nestola[2], Zengqian Hou[1], Xiangping Gu[3], Guochen Dong[1], Zhusen Yang[4], Guang Fan[5], Zhibin Xiao[6], and Kai Qu[6,7]

[1]School of Earth Sciences and Resources, China University of Geosciences, Beijing, 100083, China
[2]Department of Geosciences, University of Padova, Padua, 35131, Italy
[3]School of Geosciences and Info-Physics, Central South University, Changsha, 410083, China
[4]Institute of Geology, Chinese Academy of Geological Sciences, Beijing 100037, China
[5]Institute of Science and Technology Information, Beijing Research Institute of Uranium Geology,
Beijing, 100029, China
[6]Tianjin Center, China Geological Survey, Tianjin, 300171, China
[7]School of Earth Sciences and Engineering, Nanjing University, Nanjing, 210023, China

Correspondence: Zenqian Hou (houzengqian@126.com) and Fabrizio Nestola (fabrizio.nestola@unipd.it)

Abstract. A second occurrence of bobtraillite is described from the Gejiu nepheline syenite, southwestern China. The extremely rare and complex boron-bearing zirconium silicate is associated with albite, orthoclase, jadeite, fluorite, andradite, titanite, as well as other REE and zirconium-bearing minerals, catapleiite, moxuanxueite, låvenite, eudialyte, britholite-(Ce), and calcioancylite-(La). The EMP and LA-ICP-MS analyses of the studied material give an empirical formula: $(Na_{9.70}Li_{0.42}K_{0.08}\square_{1.80})_{\Sigma 12.00}(Sr_{10.61}Ca_{1.14}Fe_{0.07}\square_{0.18})_{\Sigma 12.00}$ $(Zr_{12.87}Ti_{0.53}Nb_{0.31}REE_{0.08}Y_{0.06}U_{0.02}Th_{0.01}\square_{0.12})_{\Sigma 14.00}(Si_{42.41}B_{5.59}Al_{0.02})_{\Sigma 48.02}O_{132}(OH)_{12} \cdot 12H_2O$. Bobtraillite is trigonal, with space group $P\bar{3}c1$, $a = 19.6977(6)$, $c = 9.9770(3)$ Å, $V = 3352.4(2)$ Å^3, $Z = 1$. Single-crystal structure refinement revealed that all sodium occupies the Na(1) and Na(2) sites; the site occupancy of these two positions is 0.835(18) and 0.15(2), respectively, suggesting that Na(1) site is Na dominant, while Na(2) is a vacancy-dominant site. The [8]-coordinated site has been assigned to Sr and Ca, with free occupancy factors, 0.874(10) and 0.126(10), respectively. These new data indicate that the ideal formula of bobtraillite could be written as $(Na,\square)_{12}(\square,Na)_{12}Sr_{12}Zr_{14}(Si_3O_9)_{10}[Si_2BO_7(OH)_2]_6 \cdot 12H_2O$.

1 Introduction

Bobtraillite is an extremely rare cyclosilicate with a unique composition and complex structure that has previously only been reported from a single locality. Only two boron-containing zirconium silicates have been found in nature so far: bobtraillite and rogermitchellite. According to the total structural information content, they are both classified into complex mineral structure (> 1000 bits per unit cell) (Grew et al., 2016); especially, rogermitchellite has the most complex crystal structure of all the boron minerals with $I_{G, \text{total}} = 3019$ bits and is the 20th most complex of the 4443 structures reported to data (Krivovichev, 2013; Krivovichev et al., 2022). The two chemically and

structurally related minerals are both found in hyperagpaitic nepheline syenites at Mont Saint-Hilaire, Quebec, Canada. The Canadian bobtraillite was originally described by McDonald and Chao (2005), the electron microprobe analyses of bobtraillite yielding an empirical formula $(Na_{11.20}Ca_{1.22})_{\Sigma 12.42}(Sr_{10.59}Ba_{0.16})_{\Sigma 10.75}(Zr_{12.69}Y_{0.63}Nb_{0.61}$ $Hf_{0.14})_{\Sigma 14.07}Si_{41.64}B_6O_{132}(OH)_{12} \cdot 12H_2O$, and the ideal formula was given as $(Na,Ca)_{13}Sr_{11}(Zr,Y,Nb)_{14}Si_{42}B_6O_{132}$ $(OH)_{12} \cdot 12H_2O$. Bobtraillite was considered as a structural hybrid of benitoite-group minerals due to its similarities in chemical composition and crystal structure. However, it is also unique among all those members for the BO_4 tetrahedra, which are linked to isolated ZrO_6 octahedra.

Although the benitoite-mineral group has only been informally defined by Hawthorne (1987), benitoite and the minerals with the structure of three-membered rings of tetrahedra have been described and discussed in previous studies (benitoite, Fischer, 1969; wadeite, Blinov et al., 1977; bazirite, Young et al., 1978; catapleiite, Ilyushin et al., 1981; and rogermitchellite, McDonald and Chao, 2010).

In this paper, we describe a second occurrence of bobtraillite from Gejiu sodalite-nepheline syenite in Yunnan Province, southwestern China. We present a detailed description of the mineral paragenesis, Raman spectroscopy, complete chemical analysis, and crystal structure refinements for the extremely rare complex zirconium silicate.

2   Occurrences and paragenesis

Bobtraillite was found in the Gejiu alkaline intrusive complex ($23°29'40''$ N, $103°4'41''$ E). This alkaline complex is associated with gabbro, granitic, and alkaline intrusions in the western part of the Cathaysia block, southwestern China (Fig. 1a). The alkaline intrusions consist mainly of early-formed silica-saturated alkali syenites from the northeastern part (Baiyunshan intrusions) and later-formed silica-undersaturated feldspathoid syenites from the northern part of the complex (Changlinggang intrusions) (Fig. 1b). The studied material is found in the feldspathoid (nepheline–sodalite) syenite. The studied material was found in hand specimen 18CL18 collected by Wang et al. (2021) near the location for their sample 18CL07. Wang et al. (2021) gave a detailed account of the geology of the Changlinggang intrusions.

Bobtraillite occurs as euhedral–subhedral granular to platy crystals, up to 100 µm in size and light brown in color. It is associated with albite, orthoclase, jadeite, fluorite, andradite, sodalite, titanite, as well as other Zr and REE-bearing minerals (catapleiite, moxuanxueite, låvenite, eudialyte, britholite-(Ce), monazite-(Ce), and calcioancylite-(La)). The complex aggregates usually form pseudomorphs of titanite or moxuanxueite in the studied thin section. The aggregates have a clear boundary between them and the surrounding albite and orthoclase (Fig. 2).

3   Raman spectroscopy

Raman spectra were collected using polished grains, and analyses were performed at Tianjin Center, China Geological Survey using a Renishaw in Via Raman microscope with a 532 nm laser (40 mW, 1 µm) and a measurement range of 4000–150 cm^{-1} (Fig. 3). In general, the medium-intensity band between 3467–3585 cm^{-1} is a superposition of O–H stretching bands of OH and H_2O. The strong and broad bands at 1522, 1766, 1989, and 2374 cm^{-1}, which are similar to the Raman spectra of other hydrous materials containing acid groups (Chukanov et al., 2022), are assigned to BO–H

stretching vibrations. These bands correspond to extremely strong hydrogen bonds in hydrated proton complexes involving proton formed as a result of partial dissociation of an acid group. The strong sharp band at 1006 cm^{-1} is assigned to v_3 (SiO_4, BO_4) antisymmetric stretching, and the weak shoulders at 983 and 1091 cm^{-1} arise from the symmetric v_1 (SiO_4, BO_4) stretching vibrations, and relatively weak peaks at 630 cm^{-1} can be identified as v_2 (SiO_4, BO_4) symmetric bending. The band at 517 cm^{-1} can be due to Zr–O stretching vibrations. The weak peak at 366 cm^{-1}, which is commonly found in the zirconium silicate, may arise from v_4 (SiO_4, BO_4) antisymmetric bending or external lattice vibrations, whereas the weak band at 201 cm^{-1} can be assigned to lattice vibrations.

4   Chemical composition

Bobtraillite was identified in the hand specimen 18CL18. The polished section 18CL18-5 was analyzed at the Beijing Research Institute of Uranium Geology with a JXA-8100 electron microprobe under operating conditions of 15 kV accelerating voltage, 10 nA beam current, and a 5 µm beam diameter. The standards used were albite (Na, Al), phlogopite (K, Fe, Mg, Si), monazite-(Ce) (P, REE, Th), plagioclase (Ca), celestite (Sr), zircon (Zr), rutile (Ti), yttrium Al garnet (Y), pure metallic Nb (Nb), and pure metallic U (U). The average of four electron microprobe analyses (wt %) is Na_2O 4.84, K_2O 0.06, SrO 17.69, CaO 1.03, FeO 0.08, MnO 0.01, Al_2O_3 0.01, ZrO_2 25.52, TiO_2 0.69, Nb_2O_5 0.66, Y_2O_3 0.11, RE_2O_3 0.23, UO_2 0.09, ThO_2 0.04, SiO_2 41.02, F 0.01, total 92.09. The content of Li_2O (0.10 %) and B_2O_3 (3.35 %) was determined by laser ablation inductively coupled plasma mass spectrometry (LA-ICP-MS) analysis. The analysis was carried out at Tianjin Center, China Geological Survey, using an Agilent 7900 equipped with a RESOlution LR laser ablation system. The operating conditions were as follows: beam diameter = 29 µm, alongside a laser pulse rate of 6 Hz with an energy density of approximately 3 J cm^{-2}. NIST SRM 610 was used for the standard. The measured content of B_2O_3 is consistent with the result (B_2O_3 3.13 %) calculated as the difference of Si + B = 48 apfu. H_2O (5.22 %) was calculated by stoichiometry from the results of the crystal structure analysis, and the hydrous nature was confirmed by means of OH stretching vibration absorption in the Raman spectrum. Complete analytical results are given in Table 1.

5   X-ray crystallography

Single-crystal X-ray studies were carried out at the School of Geosciences and Info-Physics, Central South University, with a Rigaku XtaLAB Synergy diffractometer and Cu$K\alpha$ radiation at 50 kV and 1 mA. The intensity data were corrected for X-ray absorption using multi-scan method, and empirical absorption correction was performed us-
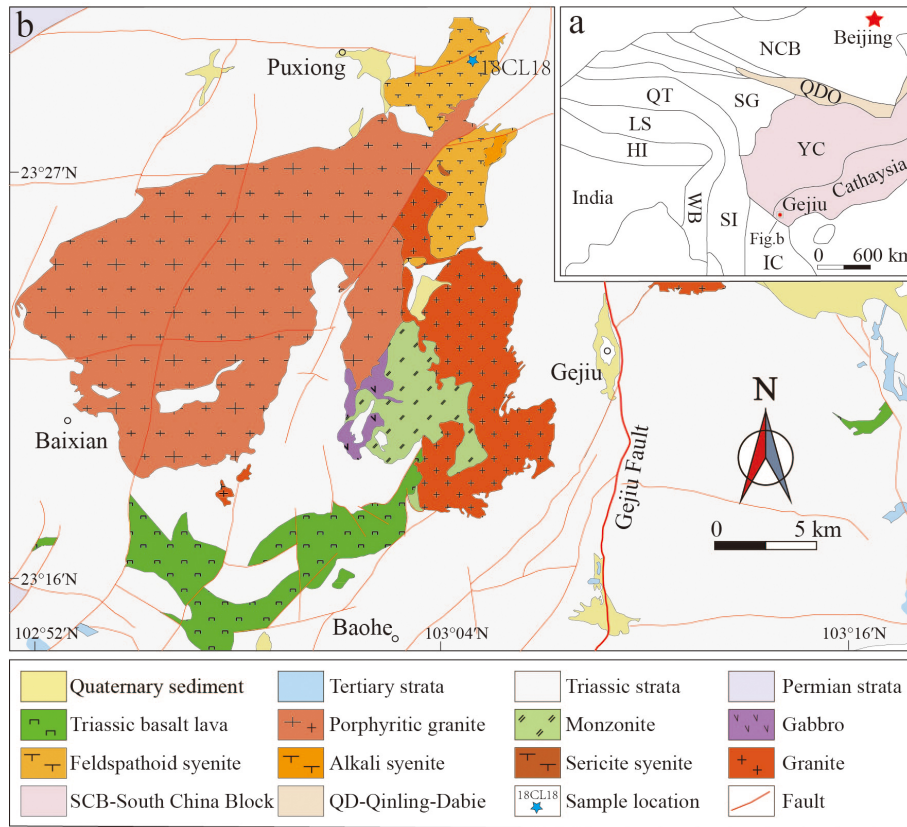
Figure 1. (a) Simplified tectonic map of eastern Asia (modified from Cheng et al., 2013); **(b)** geological map of the Gejiu, Yunnan (modified from Chen, 2019; Wang et al., 2019, 2021). NCB: North China Craton; QDO: Qinling–Dabie Orogen; IC: Indo-China Block; SI: Sibumasu Block; WB: West Burma; LS: Lhasa; QT: Qiangtang; SG: Songpan–Ganze Accretionary Complex; Hi: Himalaya.
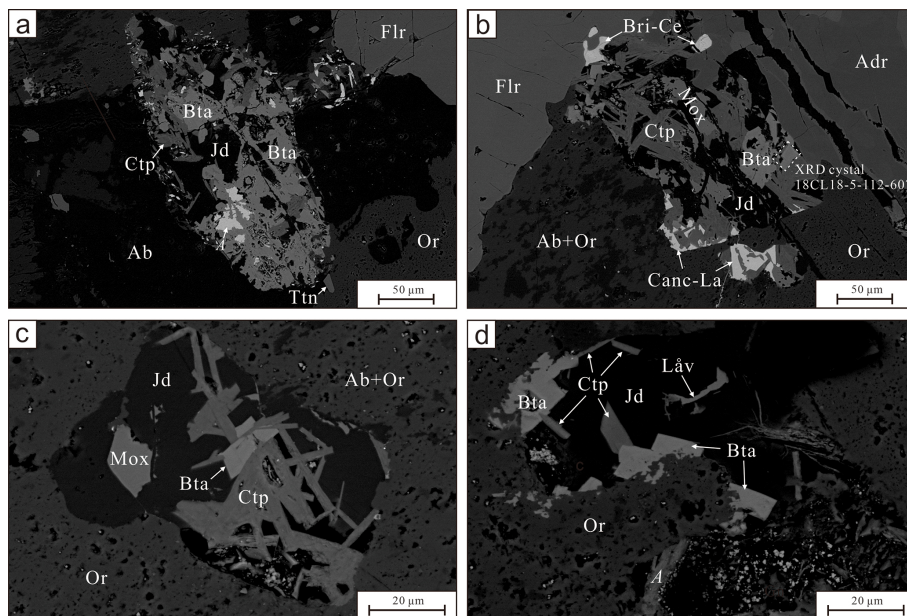
Figure 2. Back scatter electron image of the occurrence and mineral association of bobtraillite. Bta: bobtraillite, Jd: jadeite, Ab: albite, Or: orthoclase, Fl: fluorite, Adr: andradite, Ttn: titanite, Ctp: catapleiite, Mox: moxuanxueite, Låv: låvenite, Bri-Ce: britholite-(Ce), and Canc-La: calcioancylite-(La). Mineral symbols are quoted from Warr (2021).
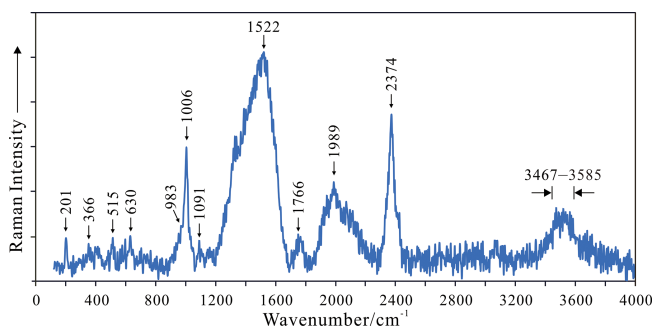
Figure 3. Raman spectrum for bobtraillite.

Table 1. Chemical data (wt %) for bobtraillite.

Constituent	Mean	Range	SD (σ)	Elem.	apfu
Li_2O	0.10			Li	0.42
Na_2O	4.84	4.64–5.04	0.18	Na	9.70
K_2O	0.06	bdl–0.13	0.05	K	0.08
CaO	1.03	0.83–1.20	0.17	Ca	1.14
SrO	17.69	17.03–18.52	0.62	Sr	10.61
FeO	0.08	bdl–0.14	0.06	Fe	0.07
MnO	0.01	bdl–0.02	0.01	Mn	0.00
Al_2O_3	0.01	bdl–0.03	0.02	Al	0.02
TiO_2	0.69	0.52–0.75	0.11	Ti	0.53
ZrO_2	25.52	24.54–25.93	0.66	Zr	12.87
Nb_2O_5	0.66	0.45–0.87	0.23	Nb	0.31
Y_2O_3	0.11	bdl–0.44	0.22	Y	0.06
La_2O_3	0.06	bdl–0.10	0.04	La	0.02
Ce_2O_3	0.03	bdl–0.07	0.03	Ce	0.01
Pr_2O_3	0.02	bdl–0.05	0.02	Pr	0.01
Nd_2O_3	0.02	bdl–0.06	0.03	Nd	0.01
Sm_2O_3	0.08	bdl–0.12	0.05	Sm	0.03
Eu_2O_3	0.02	bdl–0.04	0.02	Eu	0.01
UO_2	0.09	bdl–0.15	0.07	U	0.02
ThO_2	0.04	bdl–0.07	0.04	Th	0.01
SiO_2	41.02	40.52–41.53	0.42	Si	42.41
B_2O_3[a]	3.13			B	5.59
F	0.01	bdl–0.02	0.01	F	0
H_2O[b]	5.22			H^+	18
Total	100.5				

Notes: [a] B_2O_3 was calculated by stoichiometry based on $Si + B = 48$; [b] H_2O was calculated by stoichiometry.

ing CrysAlisPro software spherical harmonics, which was implemented in SCALE3 ABSPACK scaling algorithm. The systematic absences suggest that for the space group $P\bar{3}c1$, the refined cell parameters are $a = 19.6977(6)$ Å, $c = 9.9770(3)$ Å, and $V = 3352.4(2)$ Å^3. The structure was solved with Olex2 (Dolomanov et al., 2009) and refined with the SHELXL-program (Sheldrick, 2015). Scattering factors for neutral atoms were used initially: Si and Zr sites were fully occupied by Si and Zr, respectively, whereas the B site was refined with B vs. Si, the Na(1) and Na(2) sites were refined with Na vs. □, and the Sr site was refined with Sr

vs. Ca. After several cycles of anisotropic refinement for all the atoms, the final R_1 was 0.0586 for 1908 independent reflections with $F_o > 4\sigma$ (F_o). Crystal data collection and refinement details are reported in Table 2. Atom coordinates and isotropic displacement parameters are given in Table 3, anisotropic displacement parameters in Table 4, and selected bond distances in Table 5. The bond-valence calculations are obtained using the bond-valence parameters of Brese and O'Keeffe (1991), in Table 6.

6 Discussion

6.1 Description of the structure

6.1.1 Role of hydrogen

The crystal structure of bobtraillite contains 12 oxygen atoms, one (OH) group and one (H_2O) group. The bond valence sums (BVSs) for the oxygen atoms [O(1), O(2), O(3)...O(12)] are closer to 2 (v.u.), while the remaining two [O(13) and O(14)] are 1.146 and 0.380 v.u. (Table 6). The lower BVS suggests that they are occupied by (OH) group and water molecules at the O(13) and O(14) sites, respectively, in agreement with the chemical data and confirmed by means of OH stretching vibration absorption in the Raman spectrum. The water group is bonded to both Na sites, while the (OH) group is bonded to Na(2) site and Sr site.

6.1.2 ZrO_6 octahedra

As described by McDonald and Chao (2005), six $[Si(1)Si(2)_2O_9]^{6-}$ rings are radially distributed around a central $Zr(2)O_6$ octahedron, and the $Zr(1)O_6$ octahedra are further joined to two SiO_4 tetrahedra from the $[Si(3)_2BO_7(OH)_2]^{5-}$ rings (Fig. 4a), resulting in the formation of a giant pinwheel-like motif (Fig. 5). A small pinwheel-like pattern is achieved by central three-membered $[Si(4)_3O_9]^{6-}$ rings linking three $Zr(1)O_6$ octahedra and three $SrO_8(OH)_2$ polyhedron together along [001]. The Zr(1) site is octahedrally coordinated by O atoms with an average ⟨Zr1–O⟩ bond distances 2.072 Å, while the Zr(2) site is octahedrally coordinated by six O(5) atoms with distances 2.073 Å. The calculated BVS of Zr(1) and Zr(2) site is 4.080 and 4.056 v.u., respectively.

6.1.3 (Si, B)O_4 tetrahedra

In the tetrahedral framework there are four SiO_4 tetrahedra and one $BO_2(OH)_2$ tetrahedron. All the tetrahedra are linked into three-membered rings: $[Si(1)Si(2)_2O_9]^{6-}$, $[Si(4)_3O_9]^{6-}$, and $[Si(3)_2BO_7(OH)_2]^{5-}$ (Fig. 4b–d).

In the crystal studied, there was a mixed occupancy by B (0.92 apfu) and Si (0.08 apfu) at the B site, while other four Si sites are fully occupied by Si. The average ⟨Si–O⟩ bond lengths range from 1.609 to 1.630 Å, and average ⟨B–O/OH⟩

Table 2. Crystallographic data and refinement results for bobtraillite.

Crystal data	
Structural formula	$Na_{11.8}Sr_{10.48}Ca_{1.52}Zr_{14}Si_{42.45}B_{5.55}O_{156}$
Formula weight	6275.96
Crystal size (μm)	$16 \times 7 \times 5$
Crystal system	trigonal
Space group	$P\bar{3}c1$ (#165)
Unit cell dimensions	$a = 19.6977(6)$ Å
	$c = 9.9770(3)$ Å
Volume	$3352.4(2)$ Å^3
Z	1
Density (calculated)	$3.109\,\mathrm{g\,cm^{-3}}$

Data collection and refinement	
Instrument	Rigaku Synergy
Radiation, wavelength, temperature	$CuK\alpha$, 1.54184 Å, 293(2) K
$F(000)$	2988
2θ range (°)	5.18 to 130.168
Total reflections	12689
Unique ref (all)	1908
Unique ref $[I > 4\sigma(I)]$	1538
R_{int}	0.0757
R_{σ}	0.0409
Range of h, k, l	$-23 \leq h \leq 20, -21 \leq k \leq 22, -11 \leq l \leq 9$
$R_1, wR_2 [F_o > 4\sigma(F_o)]$	$R_1 = 0.0586, wR_2 = 0.1168$
R_1, wR_2 [all data]	$R_1 = 0.0782, wR_2 = 0.1241$
Goodness of fit	1.236
Data/restraints/parameters	1908/0/198
Maximum and minimum residual peak (e Å^{-3})	1.23 [0.90 Å from Zr(2)]
	-0.63 [2.19 Å from O13]

bond distance is 1.499 Å. The BVS calculated for Si and B are within error the same as the ideal values (Table 6).

6.1.4 $NaO_6(OH, H_2O)_2$ polyhedra

Na was assigned to individual Na(1) and Na(2) sites and forms two kinds of [8]-coordinated polyhedra: $Na(1)O_6(H_2O)_2$ and $Na(2)O_6(OH)(H_2O)$. The site occupancy of Na ions in the two Na positions was 0.835(18) and 0.15(2), respectively, suggesting 0.165 □ at Na(1) site and 0.85 □ at Na(2). The Na(1) site is coordinated by six O atoms, and two (H_2O) groups, with six long Na–O bond lengths ranging from 2.578(8) to 2.646(8) Å, and two short distances [O(14), water molecules] ranging from 2.379(11) to 2.407(11) Å. The Na(2) site is coordinated by six O atoms, one (OH) group [O(13)], and one (H_2O) group [O(14)], with six long Na(2)–O bond lengths ranging from 2.51(4) to 2.72(3) Å; the Na(2)–OH and Na(2)–H_2O bond length is 2.49(3) and 2.28(4) Å, respectively. The two Na(1) sites and one Na(2) site are connected to form a three-membered ring and are connected to the $[Si(1)Si(2)_2O_9]^{6-}$ ring. The channel generated by the overlapping rings is occupied by water molecule [O(14)] (Fig. 4b). The BVS calculated for

Na(1) and Na(2) site is 0.889 and 0.157 v.u., respectively, in perfect agreement with their refined occupancies. Interestingly, when we quantitatively analyzed the B content in bobtraillite, we unexpectedly discovered that Li is also present, which was not analyzed in the bobtraillite from Mont Saint-Hilaire. It successfully explains the insufficient cations in the Na site of bobtraillite from Gejiu syenite.

6.1.5 $SrO_8(OH)_2$ polyhedra

The Sr cation is bound to eight oxygen atoms and two hydroxyl groups to form $SrO_8(OH)_2$ polyhedra, with eight short bonds ranging from 2.524(5) to 2.737(6) Å (mean distance 2.671 Å) and two long distances (3.277, 3.279 Å). The longer bonds have also been observed in the benitoite-related minerals, for example, benitoite, pabstite, and bazirite (Hawthorne, 1987). Ten-fold coordination leads to a BVS of 1.853 v.u. for the Sr site, which decreases to 1.769 disregarding the two longest bonds. The $SrO_8(OH)_2$ polyhedron links to $[Si(4)_3O_9]^{6-}$ ring by sharing O(10) and to the $Zr(1)O_6$ octahedra via their common vertex, which forms a three-dimensional structure in single cell unit (Fig. 4d).

Table 3. Atomic coordinates and isotropic displacement parameters (in $\mathring{A}^2$) for bobtraillite.

Atom	s.o.f.	x	y	z	U_{eq}
Na1	0.835(18)	0.2182(2)	0.1096(3)	1.0002(4)	0.0339(19)
Na2	0.15(2)	0.3297(15)	0.66003(18)	0.8522(2)	0.0174(7)
Sr3	0.874(10)	0.56372(6)	0.12754(5)	0.49997(8)	0.0187(4)
Ca3	0.126(10)	0.56372(6)	0.12754(5)	0.49997(8)	0.0187(4)
Zr1		0.43385(4)	0.21697(5)	0.49998(5)	0.0132(3)
Zr2		0	0	1/2	0.0119(4)
Si1		0.12995(16)	0.12995(16)	3/4	0.0164(7)
Si2		0.30754(13)	0.21927(13)	0.7499(2)	0.0142(5)
Si3		0.43590(14)	0.34854(12)	0.2500(2)	0.0130(5)
Si4		0.57038(12)	0.25668(13)	0.2497(2)	0.0114(5)
Si5	0.08(2)	0.5187(6)	0.5187(6)	1/4	0.024(5)
B5	0.92(2)	0.5187(6)	0.5187(6)	1/4	0.024(5)
O1		0.5230(3)	0.2155(3)	0.1156(5)	0.0165(13)
O2		0.5227(3)	0.2156(3)	0.3846(5)	0.0148(12)
O3		0.3484(4)	0.2169(4)	0.6155(6)	0.0273(15)
O4		0.2185(3)	0.1429(3)	0.7497(7)	0.0228(14)
O5		0.0879(4)	0.0877(4)	0.6146(7)	0.0314(16)
O6		0.4417(4)	0.3085(4)	0.3874(6)	0.0240(15)
O7		0.4414(3)	0.3086(4)	0.1129(6)	0.0217(14)
O8		0.3483(4)	0.2168(4)	0.8850(6)	0.0290(15)
O9		0.5109(3)	0.4390(3)	0.2505(6)	0.0198(13)
O10		0.5999(3)	0.3509(3)	0.2498(6)	0.0191(13)
O11		0.3566(4)	0.3566(4)	1/4	0.0161(18)
O12		0.2972(5)	0.2972(5)	3/4	0.024(2)
O13		0.5577(4)	0.5578(4)	0.3790(6)	0.0239(15)
O14		0.2250(6)	−0.0003(6)	0.9108(10)	0.067(3)

s.o.f. – site occupancy factor.
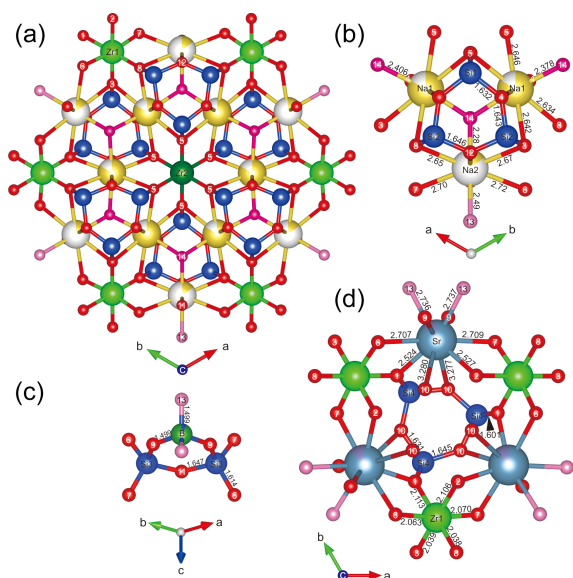
Figure 4. The crystal structure for bobtraillite (Na ions shown in yellow, Sr in gray, O in red, OH in pink, H_2O in cherry red, and vacancy in white).
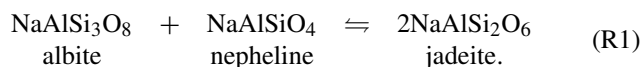
6.2　Ideal formula

The empirical formula of bobtraillite from Gejiu syenite was calculated on the basis of 156 O atoms per formula unit (apfu); B content was calculated as the difference of $Si + B = 48$ apfu; H content was estimated by stoichiometry in order to achieve the electrostatic balance. The studied material corresponds to the chemical formula $(Na_{9.70}Li_{0.42}$ $K_{0.08})_{\sum 10.20}(Sr_{10.61}Ca_{1.14}Fe_{0.07})_{\sum 11.82}(Zr_{12.87}Ti_{0.53}Nb_{0.31}$ $RE_{0.14}U_{0.02}Th_{0.01})_{\sum 13.88}(Si_{42.41}B_{5.59}Al_{0.02})_{\sum 48.02}O_{132}$ $(OH)_{12} \cdot 12H_2O$. Differently from previous studies (McDonald and Chao, 2005), if we introduce a small number of divalent calcium ions into the two Na sites of our studied material, the R value increases. In addition, we are confident in stating that our BVS calculation is in agreement with the absence of Ca at the two Na sites. Instead, all the Ca is substituting for Sr at the Sr site. Taking into account the results of the crystal structure refinement, the ideal end-member formula of bobtraillite could be written as $(Na, \square)_{12}(\square,$ $Na)_{12}Sr_{12}Zr_{14}(Si_3O_9)_{10}[Si_2BO_7(OH)_2]_6 \cdot 12H_2O$. In order to keep the charge balance of the end-member formula, the total site population of Na is set to 10 apfu, ideally correspondingto (wt %) Na_2O 4.89, SrO 19.63, ZrO_2 29.40, SiO_2 25.16, B_2O_3 3.30, H_2O 5.12, and a total of 100.

Table 4. Anisotropic displacement parameters (in $\mathring{A}^2$) for bobtraillite.

Atom	U_{11}	U_{22}	U_{33}	U_{23}	U_{13}	U_{12}
Na1	0.031(3)	0.034(3)	0.033(3)	0.014(2)	0.001(2)	0.014(2)
Na2	0.021(17)	0.031(17)	0.05(2)	−0.022(12)	0.010(12)	0.002(13)
Sr3	0.0182(5)	0.0207(5)	0.0179(5)	0.0000(3)	0.0010(3)	0.0102(4)
Ca3	0.0182(5)	0.0207(5)	0.0179(5)	0.0000(3)	0.0010(3)	0.0102(4)
Zr1	0.0149(4)	0.0156(4)	0.0093(4)	0.0005(3)	−0.0001(2)	0.0077(3)
Zr2	0.0139(5)	0.0139(5)	0.0080(7)	0	0	0.0069(3)
Si1	0.0159(12)	0.0159(12)	0.0144(15)	0.0001(7)	−0.0001(7)	0.0058(14)
Si2	0.0142(11)	0.0168(12)	0.0116(11)	0.0005(9)	0.0004(8)	0.0078(9)
Si3	0.0165(12)	0.0124(11)	0.0119(11)	−0.0008(8)	0.0005(8)	0.0086(9)
Si4	0.0122(11)	0.0107(11)	0.0108(10)	0.0001(8)	0.0009(8)	0.0053(9)
Si5	0.023(7)	0.023(7)	0.032(7)	0.001(2)	−0.001(2)	0.015(6)
B5	0.023(7)	0.023(7)	0.032(7)	0.001(2)	−0.001(2)	0.015(6)
O1	0.019(3)	0.020(3)	0.012(3)	−0.001(2)	−0.006(2)	0.011(2)
O2	0.019(3)	0.019(3)	0.011(3)	0.005(2)	0.008(2)	0.013(2)
O3	0.037(4)	0.035(4)	0.015(3)	0.002(3)	0.006(3)	0.022(3)
O4	0.015(3)	0.016(3)	0.039(4)	−0.002(3)	−0.002(3)	0.008(3)
O5	0.030(4)	0.030(4)	0.025(3)	−0.006(3)	−0.006(3)	0.007(3)
O6	0.028(4)	0.022(3)	0.023(3)	0.007(3)	0.003(3)	0.014(3)
O7	0.027(3)	0.022(3)	0.019(3)	−0.006(2)	0.001(2)	0.014(3)
O8	0.035(4)	0.036(4)	0.022(4)	0.000(3)	−0.007(3)	0.023(3)
O9	0.011(3)	0.018(3)	0.031(3)	−0.001(3)	−0.002(2)	0.007(2)
O10	0.016(3)	0.006(3)	0.032(3)	0.000(2)	−0.002(2)	0.004(2)
O11	0.015(3)	0.015(3)	0.019(4)	0.0015(16)	−0.0015(16)	0.007(4)
O12	0.023(3)	0.023(3)	0.025(5)	0.0003(19)	−0.0003(19)	0.010(4)
O13	0.022(3)	0.025(3)	0.024(3)	0.003(3)	−0.001(3)	0.011(3)
O14	0.080(7)	0.059(6)	0.056(6)	0.000(5)	0.013(5)	0.032(5)

6.3 Genesis of bobtraillite

Although only two occurrences of bobtraillite have been reported so far, it is almost certainly a secondary mineral. This is strongly demonstrated in the original description of bobtraillite from the type locality by McDonald and Chao (2005); there it is very clearly shown that fine-grained bobtraillite, associated with other secondary carbonates and other hydrous minerals, occurs in cavities in the early-formed alkaline breccias. In our case, bobtraillite occurs in the fine- to coarse-grained nepheline–sodalite syenites. The assemblages where bobtraillite occurs usually form pseudomorphs of titanite or moxuanxueite, indicating it is the decomposition product of the primary minerals. It should be noted that jadeite usually occurs in the central part of the aggregates (Fig. 2), indicating bobtraillite formed at the same stage, and thus the jadeite should play a key role in discussing the alteration process. In silica-undersaturated rocks, where jadeite could form through the following Reaction (R1) given by Boettcher and Wyllie (1968):

$$\underset{\text{albite}}{\text{NaAlSi}_3\text{O}_8} + \underset{\text{nepheline}}{\text{NaAlSiO}_4} \rightleftharpoons \underset{\text{jadeite.}}{2\text{NaAlSi}_2\text{O}_6} \qquad \text{(R1)}$$

The Reaction (R1) between nepheline and albite to produce jadeite is in the presence of excess H_2O (Gupta, 2015). This is consistent with the observed albite always occur-
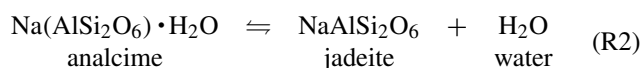
ring around mineral pseudomorph assemblage in the later-formed silica-undersaturated feldspathoid syenites from the Changlinggang intrusions. Previous studies have experimentally confirmed that this jadeite could form at a lower pressure in silica-undersaturated rocks than in silica-saturated rocks (Popp and Gilbert, 1972). Andersen et al. (2010) suggested that catapleiite could replace primary zirconium minerals under a relatively high H_2O activity environment. The increasing activity of water can also be substantiated by the replacement of primary anhydrous moxuanxueite by late-formed hydrous bobtraillite and catapleiite. This process could occur at a relatively low temperature ($\leq 348\,^\circ$C) (Chakrabarty et al., 2016), which is significantly lower than the magma crystallization temperature of Gejiu feldspathoid syenites ($898\,^\circ$C) (Wang et al., 2021).

In addition, jadeite could also form from the breakdown of analcime according to the Reaction (R2) given by Kennedy (1961). The reaction could explain the paucity of hydrous analcime in the Gejiu feldspathoid syenites within the hydrothermal assemblage. The release of H_2O, with the Ca, Sr, and Zr elements released from the breakdown of moxuanxueite to form the secondary hydrous zirconium silicates, for example, bobtraillite and catapleiite. It is worth noting that analcime is considered a decomposition product of nepheline (Henderson and Gibb, 1977). That means there are at least two stages of hydrothermal process. The first stage is

Table 5. Selected bond lengths (Å) for bobtraillite.

Na1	–O14	2.379(11)	Na2	–O14	2.28(4)
	–O14′	2.407(11)		–O13	2.49(3)
	–O4	2.578(8)		–O12	2.51(4)
	–O4′	2.583(8)		–O11	2.62(4)
	–O8	2.634(8)		–O8	2.65(3)
	–O3	2.643(8)		–O3	2.67(3)
	–O5	2.645(8)		–O7	2.70(3)
	–O5′	2.646(8)		–O6	2.72(3)
mean		**2.564(9)**	**mean**		**2.58(3)**
Sr3	–O1	2.524(5)	Zr1	–O8	2.038(6)
	–O2	2.527(5)		–O3	2.040(6)
	–O6	2.707(6)		–O6	2.063(6)
	–O7	2.709(6)		–O7	2.070(6)
	–O9	2.709(6)		–O2	2.107(5)
	–O9′	2.719(6)		–O1	2.113(5)
	–O13	2.736(6)	**mean**		**2.072(6)**
	–O13′	2.737(6)			
	–O10	3.277(6)	Zr2	–O5$^{\times 6}$	2.073(6)
	–O10′	3.279(6)			
Mean[8]		**2.671(6)**			
Mean[10]		**2.792(6)**	Si2	–O3	1.577(6)
				–O8	1.582(7)
Si1	–O5$^{\times 2}$	1.586(7)		–O4	1.644(6)
	–O4$^{\times 2}$	1.632(6)		–O12	1.646(4)
mean		**1.609(7)**	**mean**		**1.612(6)**
Si3	–O7	1.609(6)	Si4	–O1	1.601(6)
	–O6	1.614(6)		–O2	1.609(5)
	–O11	1.647(4)		–O10	1.631(6)
	–O9	1.651(6)		–O10′	1.631(6)
mean		**1.630(6)**	**mean**		**1.618(6)**
B5	–O9$^{\times 2}$	1.498(9)			
	–O13$^{\times 2}$	1.499(9)			
mean		**1.499(9)**			

mineral assemblages resemble those in the Gejiu alkaline intrusive complex. The possibility of Li enrichment in hyperagpaitic intrusive complexes reminds us that cation-deficient minerals in such rocks, which have only been analyzed by the electron microprobe, need to be checked for Li, Be, and B, constituents that either cannot be analyzed with the electron microprobe or analyzed only with great difficulty. These under-reported light elements often play a crucial role in ore-forming processes during the late stages of magmatic crystallization (Alferyeva et al., 2011).

the replacement of primary nepheline and alkali feldspar by analcime, and then the secondary analcime continues to alter to jadeite.

$$\underset{\text{analcime}}{\text{Na(AlSi}_2\text{O}_6)\cdot\text{H}_2\text{O}} \rightleftharpoons \underset{\text{jadeite}}{\text{NaAlSi}_2\text{O}_6} + \underset{\text{water}}{\text{H}_2\text{O}} \quad \text{(R2)}$$

The source of the B is still an open question. However, another boron silicate (stillwellite) has been found in both the Gejiu and the Mont Saint-Hilaire hyperagpaitic syenites (McDonald and Chao, 2005), which is considered to crystallize during the late pegmatitic and succeeding hydrothermal stages (Bailey, 2006; Chakrabarty et al., 2016). Furthermore, Li may be a more abundant constituent in hyperagpaitic rocks than is commonly realized. The Gejiu nepheline–sodalite syenite contains 107 ppm Li$_2$O (Wang et al., 2021), and several lithium minerals have been found associated with the hyperagpaitic intrusions at Mont Saint-Hilaire (Van Velthuizen and Chao, 1989; Khomyakov et al., 1990; Chao et al., 1991; Chao and Ercit, 1991; McDonald et al., 2013), where the

Table 6. Bond-valence calculation for bobtraillite.

	Na1	Na2	Sr	Zr1	Zr2	Si1	Si2	Si3	Si4	B	Total
O1			0.320	0.607					1.064		1.991
O2			0.317	0.616					1.041		1.974
O3	0.086	0.014		0.739			1.135				1.974
O4	0.101 0.103					$0.979^{\times2\downarrow}$	0.947				2.130
O5	0.086 0.086				$0.676^{\times6\downarrow}$	$1.108^{\times2\downarrow}$					1.956
O6		0.013	0.195	0.694				1.027			1.929
O7		0.013	0.194	0.681				1.041			1.929
O8	0.088	0.015		0.743			1.12				1.966
O9			0.194 0.189					0.93		$0.765^{\times2\downarrow}$	2.078
O10			0.042 0.042						$0.981^{\times2\downarrow}$ $0.945^{\times2\downarrow}$		2.010
O11		$0.016^{\times2\rightarrow}$						$0.94^{\times2\rightarrow}$			1.912
O12		$0.022^{\times2\rightarrow}$					$0.942^{\times2\rightarrow}$				1.928
O13		0.023	0.180 0.180							$0.763^{\times2\downarrow}$	1.146
O14	0.163 0.176	0.041									0.380
Total	0.889	0.157	1.853	4.080	4.056	4.174	4.144	3.938	4.031	3.056	

Notes: bond valence sums were calculated with the site-occupancy factors given in Table 4. Calculations were done using the equation and constants of Brown (1977), $S = \exp[(R_0 - d_0)/b]$.
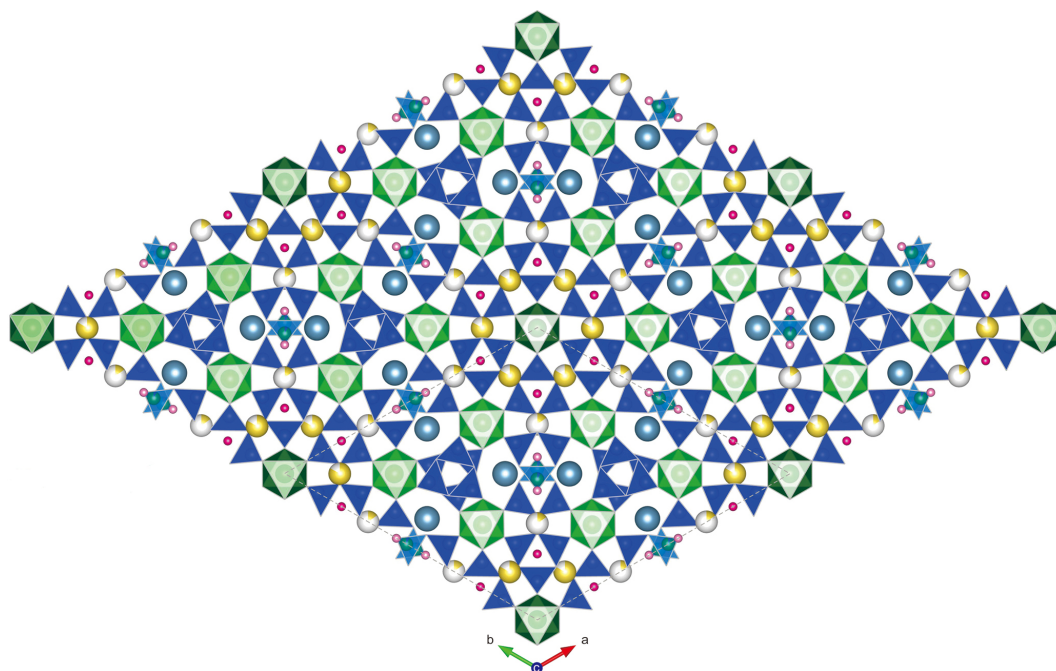
Figure 5. The giant pinwheel motif view of bobtraillite along [001] (four-unit cells, the dotted line is a single unit cell). The $Zr(1)O_6$ octahedra are shown in green, the $Zr(2)O_6$ octahedra in olive green, the SiO_4 tetrahedra in indigo, and BO_4 tetrahedra in green-blue. Other legends as in Fig. 4.

References

Alferyeva, Y. O., Gramenitskii, E. N., and Shchekina, T. I.: Experimental study of phase relations in a lithium-bearing fluorine-rich haplogranite and nepheline syenite system, Geochem. Int., 49, 676–690, 2011.

Andersen, T., Erambert, M., Larsen, A. O., and Selbekk, R. S.: Petrology of nepheline syenite pegmatites in the Oslo Rift, Norway: Zirconium silicate mineral assemblages as indicators of alkalinity and volatile fugacity in mildly agpaitic magma, J. Petrol., 51, 2303–2325, 2010.

Bailey, J. C.: Geochemistry of boron in the Ilímaussaq alkaline complex, South Greenland, Lithos, 91, 319–330, 2006.

Blinov, V. A., Shumyatskaya, N. G., Voronkov, A. A., Ilyukhin, V. V., and Belov, N. V.: Refinement of the crystal structure of wadeite $K_2Zr[Si_3O_9]$ and its relationship to kindred structural types, Sov. Phys. Crystallogr., 22, 31–35, 1977.

Boettcher, A. L. and Wyllie, P. J.: Jadeite stability measured in the presence of silicate liquids in the system $NaAlSiO_4$–SiO_2–H_2O, Geochim. Cosmochim. Ac., 32, 999–1012, 1968.

Brese, N. E. and O'Keeffe, M.: Bond-valence parameters for solids, Acta Crystallogr. B, 47, 192–197, 1991.

Brown, I. D.: Predicting bond lengths in inorganic crystals, Acta Crystallogr. B, 33, 1305–1310, 1977.

Chakrabarty, A., Mitchell, R. H., Ren, M., Saha, P. K., Pal, S., Pruseth, K. L., and Sen, A. K.: Magmatic, hydrothermal and subsolidus evolution of the agpaitic nepheline syenites of the Sushina Hill Complex, India: implications for the metamorphism of peralkaline syenites, Mineral. Mag., 80, 1161–1193, 2016.

Chao, G. Y. and Ercit, T. S.: Nalipoite, sodium dilithium phosphate, a new mineral species from Mont Saint-Hilaire, Quebec, Can. Mineral., 29, 565–568, 1991.

Chao, G. Y., Grice, J. D., and Gault, R. A.: Silinaite, a new sodium lithium silicate hydrate mineral from Mont Saint-Hilaire, Quebec, Can. Mineral., 29, 359–362, 1991.

Chen, W.: The granitic magmatism and its significance of mineralization in Gejiu, Yunnan, Master Dissertation, China University of Geosciences (Beijing), 1–63, https://doi.org/10.27493/d.cnki.gzdzy.2019.001372, 2019 (in Chinese with English abstract).

Cheng, Y. B., Mao, J. W., and Spandler, C.: Petrogenesis and geodynamic implications of the Gejiu igneous complex in the western Cathaysia block, South China, Lithos, 175, 213–229, 2013.

Chukanov, N. V., Vigasina, M. F., Rastsvetaeva, R. K., Aksenov, S. M., Mikhailova, J. A., and Pekov, I. V.: The evidence of hydrated proton in eudialyte-group minerals based on Raman spectroscopy data, J. Raman. Spectroc., 53, 1188–1203, 2022.

Dolomanov, O. V., Bourhis, L. J., Gildea, R. J, Howard, J. A. K., and Puschmann, H.: OLEX2: A complete structure solution, refinement and analysis program, J. Appl. Crystallogr., 42, 339–341, 2009.

Fischer, K.: Verfeinerung der Kristallstruktur yon Benitoit $BaTi[Si_3O_9]$, Z. Kristallogr., 129, 222–243, 1969.

Grew, E. S., Krivovichev, S. V., Hazen, R. M., and Hystad, G.: Evolution of structural complexity in boron minerals, Can. Mineral., 54, 125–143, 2016.

Gupta, A. K. (Ed.): Ternary systems with feldspathoids, in: Origin of Potassium-rich Silica-deficient Igneous Rocks, Springer, New Delhi, 259–276, https://doi.org/10.1007/978-81-322-2083-1_7, 2015.

Hawthorne, F. C.: The crystal chemistry of the benitoite group minerals and structural relations in (Si_3O_9) ring structures, Neues Jb. Miner. Monat., 1, 16–30, 1987.

Henderson, C. M. B. and Gibb, F. G. F.: Formation of analcime in the Dippin Sill, Isle of Arran, Mineral. Mag., 41, 534–537, 1977.

Ilyushin, G. D., Voronkov, A. A., Ilyukhin, V. V., Nevskii, N. N., and Belov, N. V.: Crystal structure of natural monoclinic catapleiite $Na_2ZrSi_3O_9 \cdot 2H_2O$, Sov. Phys. Dokl. 26, 808–809, 1981.

Kennedy, G. C.: Phase relations of some rocks and minerals at high temperatures and high pressures, Adv. Geophys., 7, 303–322, 1961.

Khomyakov, A. P., Polezhaeva L. I., Merlino, S., and Pasero, M.: Lintisite, $Na_3LiTiSi_4O_{14} \cdot 2H_2O$ – a new mineral, Zapinski Vsesoyuznogo Mineralogicheskogo Obshchestva, 119, 76–80, 1990.

Krivovichev, S. V.: Structural complexity of minerals: information storage and processing in the mineral world, Mineral. Mag., 77, 275–326, 2013.

Krivovichev, S. V., Krivovichev, V. G., Hazen, R. M., Aksenov, S. M., Avdontceva, M. S., Banaru, A. M., Gorelova, L. A., Ismagilova, R. M., Kornyakov, I. V., Kuporev, I. V., Morrison, S. M., Panikorovskii, T. L., and Starova, G. L.: Structural and chemical complexity of minerals: an update, Mineral. Mag., 86, 183–204, 2022.

McDonald, A. M. and Chao, G. Y.: Bobtraillite, $(Na, Ca)_{13}Sr_{11}(Zr, Y, Nb)_{14}Si_{42}B_6O_{132}(OH)_{12} \cdot 12H_2O$, a new mineral species from Mont Saint-Hilaire, Quebec: Description, structure determination and relationship to benitoite and wadeite, Can. Mineral., 43, 747–758, 2005.

McDonald, A. M. and Chao, G. Y.: Rogermitchellite, $Na_{12}(Sr, Na)_{24}Ba_4Zr_{26}Si_{78}(B, Si)_{12}O_{246}(OH)_{24} \cdot 18H_2O$, a new mineral species from Mont Saint-Hilaire, Quebec: Description, structure determination and relationship with HFSE-bearing cyclosilicates, Can. Mineral., 48, 267–278, 2010.

McDonald, A. M., Back, M. E., Gault, R. A., and Horváth, L.: Peatite-(Y) and ramikite-(Y), two new Na-Li-Y ± Zr phosphate-carbonate minerals from the Poudrette pegmatite, Mont Saint-Hilaire, Québec, Can. Mineral., 51, 569–596, 2013.

Popp, R. K. and Gilbert, M. C.: Stability of acmite-jadeite pyroxene at low pressure, Am. Miner., 57, 1210–1231, 1972.

Sheldrick, G. M.: Crystal structure refinement with SHELXL, Acta Crystallogr. C, 71, 3–8, 2015.

Van Velthuizen, J. and Chao, G. Y.: Griceite, LiF, a new mineral species from Mont Saint-Hilaire, Quebec, Can. Mineral., 27, 125–127, 1989.

Wang, Y. F., Dong, G. C., Chen, W., Su, L., Yin, G. D., Zhu, H. Y., and Li, H. W.: Characteristics and petrogenesis of feldspathoid syenite in Gejiu, Yunnan, Earth Sci. Front., 26, 209–220, 2019 (in Chinese with English abstract).

Wang, Y. F., Dong, G. C., Santosh, M., Liu, C., Chen, W., Liang, J. L., and Zhang, Y. C.: Alkaline magmatism on Neo-Tethyan extensional domains: Evidences from the Gejiu complex in Yunnan, China, Geol. J., 56, 4331–4348, 2021.

Warr, L. N.: IMA–CNMNC approved mineral symbols, Mineral. Mag., 85, 291–320, 2021.

Young, B. R., Hawkes, J. R., Merriman, R. J., and Styles, M. T.: Bazirite, $BaZrSi_3O_9$, a new mineral from Rockall Island, Inverness-shire, Scotland, Mineral. Mag., 42, 35–40, 1978.